Search for Light Gluinos via Decays Containing $\pi^+\pi^-$ or π^0 from a Neutral Hadron Beam at Fermilab

A. Alavi-Harati,[12] I. F. Albuquerque,[10] T. Alexopoulos,[12] M. Arenton,[11] K. Arisaka,[2] S. Averitte,[10] A. R. Barker,[5] L. Bellantoni,[7] A. Bellavance,[9] J. Belz,[10] R. Ben-David,[7] D. R. Bergman,[10] E. Blucher,[4] G. J. Bock,[7] C. Bown,[4] J. D. Bricker,[10] S. Bright,[4] E. Cheu,[1] S. Childress,[7] R. Coleman,[7] M. D. Corcoran,[9] G. Corti,[11] B. Cox,[11] M. B. Crisler,[7] A. R. Erwin,[12] R. Ford,[7] A. Golossanov,[11] G. Graham,[4] J. Graham,[4] K. Hagan,[11] E. Halkiadakis,[10] K. Hanagaki,[8] S. Hidaka,[8] Y. B. Hsiung,[7] V. Jejer,[11] J. Jennings,[2] D. A. Jensen,[7] R. Kessler,[4] H. G. E. Kobrak,[3] J. LaDue,[5] A. Lath,[10,*] A. Ledovskoy,[11] P. L. McBride,[7] A. P. McManus,[11] P. Mikelsons,[5] E. Monnier,[4,†] T. Nakaya,[7] U. Nauenberg,[5] K. S. Nelson,[11] H. Nguyen,[7] V. O'Dell,[7] M. Pang,[7] R. Pordes,[7] V. Prasad,[4] C. Qiao,[4] B. Quinn,[4] E. J. Ramberg,[7] R. E. Ray,[7] A. Roodman,[4] M. Sadamoto,[8] S. Schnetzer,[10] K. Senyo,[8] P. Shanahan,[7] P. S. Shawhan,[4] W. Slater,[2] N. Solomey,[4] S. V. Somalwar,[10] R. L. Stone,[10] I. Suzuki,[8] E. C. Swallow,[4,6] R. A. Swanson,[3] S. A. Taegar,[1] R. J. Tesarek,[10] G. B. Thomson,[10] P. A. Toale,[5] A. K. Tripathi,[2] R. Tschirhart,[7] Y. W. Wah,[4] J. Wang,[1] H. B. White,[7] J. Whitmore,[7] B. Winstein,[4] R. Winston,[4] J.-Y. Wu,[5] T. Yamanaka,[8] and E. D. Zimmerman[4]

(KTeV Collaboration)

[1]*University of Arizona, Tucson, Arizona 85721*
[2]*University of California at Los Angeles, Los Angeles, California 90095*
[3]*University of California at San Diego, La Jolla, California 92093*
[4]*The Enrico Fermi Institute, The University of Chicago, Chicago, Illinois 60637*
[5]*University of Colorado, Boulder, Colorado 80309*
[6]*Elmhurst College, Elmhurst, Illinois 60126*
[7]*Fermi National Accelerator Laboratory, Batavia, Illinois 60510*
[8]*Osaka University, Toyonaka, Osaka 560, Japan*
[9]*Rice University, Houston, Texas 77005*
[10]*Rutgers University, Piscataway, New Jersey 08855*
[11]*University of Virginia, Charlottesville, Virginia 22901*
[12]*University of Wisconsin, Madison, Wisconsin 53706*
(Received 18 March 1999)

We report on two null searches, one for the spontaneous appearance of $\pi^+\pi^-$ pairs, another for a single π^0, consistent with the decay of a long-lived neutral particle into hadrons and an unseen neutral particle. For the lowest level gluon-gluino bound state, known as the R^0, we exclude the decays $R^0 \to \pi^+\pi^-\tilde{\gamma}$ and $R^0 \to \pi^0\tilde{\gamma}$ for the masses of R^0 and $\tilde{\gamma}$ in the theoretically allowed range. In the most interesting R^0 mass range, ≤ 3 GeV$/c^2$, we exclude R^0 lifetimes from 3×10^{-10} sec to as high as 10^{-3} sec, assuming perturbative QCD production for the R^0.

PACS numbers: 13.85.Rm, 14.80.Ly

Light masses for gluinos ($\tilde{g}$) and photinos ($\tilde{\gamma}$) arise naturally in many supersymmetry (SUSY) models, including those that solve the SUSY-CP problem by eliminating dimension-3 operators [1]. They predict light gauginos and heavy squarks, and have not been ruled out conclusively. In such models the gluino and photino masses are expected to be ≤ 1.0 GeV$/c^2$. The gluino should form bound states with normal quarks and gluons (g), the lightest of which is called the R^0, a spin $1/2\, g\tilde{g}$ bound state.

Estimates of the mass and lifetime of the R^0 vary from 1 to 3 GeV$/c^2$ and 10^{-10} to 10^{-5} sec, respectively [2]. Chung, Farrar, and Kolb [3] show that a stable $\tilde{\gamma}$ as a relic dark matter candidate requires the ratio of masses $M_{R^0}/M_{\tilde{\gamma}} \equiv r$ to be $1.3 \leq r \leq 1.8$. The range $1.3 \leq r \leq 1.55$ is favored. Values of r below 1.3 yield an insufficient abundance of dark matter, while too large a value of r overcloses the universe. A previous direct search for the R^0 by the KTeV Collaboration is described in [4]. That result, based on 5% of the data collected by the KTeV experiment in 1996, excluded the R^0 with the constraint $M_{R^0} - M\tilde{\gamma} \geq 0.648$ GeV$/c^2$. Thus for $r \leq 1.4$, our previous result was insensitive to $M_{R^0} \leq 2.3$ GeV$/c^2$, which represents a large portion of the region of primary interest [5]. A search for the C-suppressed decay $R^0 \to \eta\tilde{\gamma}$ is discussed in [6]. References to other searches can be found in [4].

We assume exactly the same production mechanism and rates as described in [4]. The R^0 is expected to decay mainly into $\rho\tilde{\gamma}$. The decay into $\pi^0\tilde{\gamma}$ or $\eta\tilde{\gamma}$ is suppressed due to conservation of C parity. Figure 1 illustrates the lower limit of sensitivity in $M_{R^0} - M_{\tilde{\gamma}}$ of the three decay modes mentioned above, along with the cosmological constraints. We report on null searches for two decay modes. The first is the dominant decay, $R^0 \to \rho\tilde{\gamma}$, $\rho \to \pi^+\pi^-$. The second is the C-violating decay $R^0 \to \pi^0\tilde{\gamma}$. In both decays, the $\tilde{\gamma}$ escapes undetected.

 © 1999 The American Physical Society

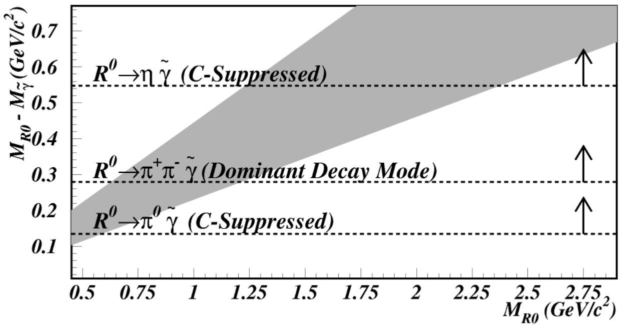

FIG. 1. $M_{R^0} - M_{\tilde{\gamma}}$ vs M_{R^0}, showing the region allowed by cosmological arguments, $1.3 \leq r \leq 1.8$ (shaded). The dashed lines represent the lowest level of sensitivity for the various decay modes.

The KTeV experiment as used in the R^0 search is described in [4]. The data used in the $R^0 \to \rho\tilde{\gamma}$, $\rho \to \pi^+\pi^-$ analysis were collected during the 1996 run of KTeV (FNAL E832). The trigger and analysis cuts used are similar to those described in [4]. To detect a possible R^0 signal we examined decays with two charged particles, specifically the shape of the invariant mass distribution, with the assumption that the particles were pions ($M_{\pi^+\pi^-}$).

An on-line filter was used during data collection to classify the events according to $\pi^+\pi^-$ invariant mass. The data with $M_{\pi^+\pi^-} < 0.45\ \mathrm{GeV}/c^2$ were prescaled. Backgrounds consisted of $K_L \to \pi^\pm l^\mp \nu$ ($l = e, \mu$) decays with leptons misidentified as pions (semileptonic decays), $K_L \to \pi^+\pi^-$ and $K_L \to \pi^+\pi^-\gamma$ decays, as well as $K_L \to \pi^+\pi^-\pi^0$ decays with undetected π^0's.

The off-line analysis, including cuts using photon veto energies, semileptonic decay rejection, and track, vertex quality requirements, was similar to that described in [4]. Additional cuts reduced the probability of track reconstruction errors that paired the wrong combination of horizontal and vertical track components. The $K_L \to \pi^+\pi^-$ decays were rejected by requiring the square of the transverse momentum of the $\pi^+\pi^-$ with respect to the beam direction (P_T^2) to be greater than 0.001 $(\mathrm{GeV}/c)^2$, and the $K_L \to \pi^+\pi^-\gamma$ and $K_L \to \pi^+\pi^-\pi^0$ decays were rejected by using the calorimeter to identify the photons from respective decays. In the region $M_{\pi^+\pi^-} \leq 0.36\ \mathrm{GeV}/c^2$ additional cuts ($K_L \to \pi^+\pi^-\pi^0$ specific cuts), including restricting the total energy deposited in the calorimeter to $\leq 5\ \mathrm{GeV}/c^2$, further reduced the $K_L \to \pi^+\pi^-\pi^0$ decays.

We performed a maximum-likelihood fit to the $M_{\pi^+\pi^-}$ distribution, using Monte Carlo (MC) distributions for $K_L \to \pi e \nu$, $K_L \to \pi\mu\nu$, $K_L \to \pi^+\pi^-$, $K_L \to \pi^+\pi^-\pi^0$, and $R^0 \to \pi^+\pi^-\tilde{\gamma}$. The Monte Carlo events were subjected to all the same cuts as the data. However, the $e^\pm$ identification cut was not applied to the $K_L \to \pi e \nu$, and a muon veto requirement was not applied to the $K_L \to \pi\mu\nu$ events, since not all the sources of lepton misidentification were simulated in our Monte Carlo. Any possible effects on the $M_{\pi^+\pi^-}$ distribution due to not applying lepton identification cuts have been studied in detail and found to be negligible. The amplitudes for all the simulated $M_{\pi^+\pi^-}$ shapes were allowed to vary independently.

Figure 2(a) shows the $M_{\pi^+\pi^-}$ distribution for all data, before applying the $K_L \to \pi^+\pi^-\pi^0$ specific and P_T^2 cuts. There are $\sim 2.1 \times 10^6$ CP-violating $K_L \to \pi^+\pi^-$ decays in the peak at M_K. The sharp edge at $M_{\pi^+\pi^-} = 0.45\ \mathrm{GeV}/c^2$ is due to the on-line filter prescale. The $K_L \to \pi^+\pi^-\pi^0$ decays are evident at $M_{\pi^+\pi^-} \leq 0.36\ \mathrm{GeV}/c^2$, and the kinematic limit is evident at $2M_\pi = 0.28\ \mathrm{GeV}/c^2$. Also shown in Fig. 2(a) is the sum of the various kaon decay distributions from Monte Carlo. The data and kaon decay simulation are in agreement for 6 orders of magnitude. In addition, the P_T^2 distributions for data and sum of decay simulations (not shown) are in good agreement, using the amplitudes for the various kaon decays found in $M_{\pi^+\pi^-}$ fit.

Figure 2(b) shows the $M_{\pi^+\pi^-}$ distribution for the data with all the cuts, as well as the sum of the K_L decay simulations, and distributions for two sample $R^0, \tilde{\gamma}$ combinations. The $K_L \to \pi^+\pi^-$ peak in data is significantly reduced due to the P_T^2 cut. The agreement between data and the sum of K_L decay simulations has an overall χ^2/degree of freedom of $\sim 194/148$ for the region $0.28 \leq M_{\pi^+\pi^-} \leq 0.58\ \mathrm{GeV}/c^2$.

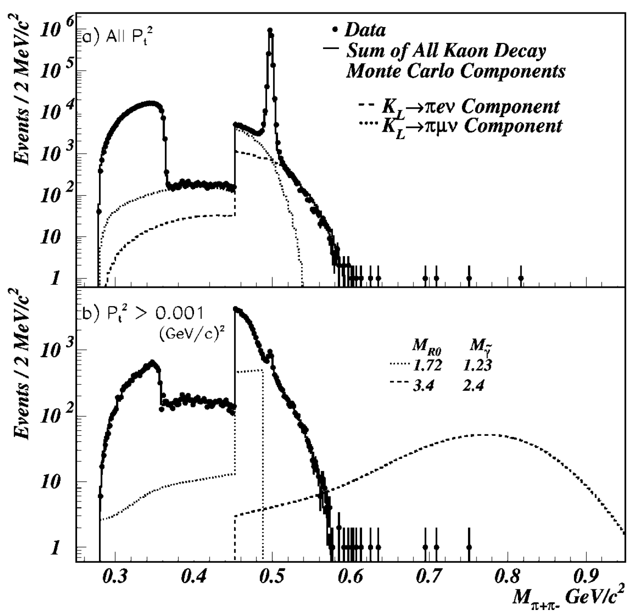

FIG. 2. $M_{\pi^+\pi^-}$ distribution with all but P_T^2 and $K_L \to \pi^+\pi^-\pi^0$ specific cuts (a), and all cuts (b). The data (dots), sum of all MC (solid line) are shown. Suppression below $0.45\ \mathrm{GeV}/c^2$ is due to the on-line filter prescale. The separate contributions from semileptonic decays (dashed and dotted lines) are also shown in (a). Distributions due to two sample R^0's of lifetime 5×10^{-8} sec using the predicted flux (dashed and dotted lines) are also shown in (b).

The two sample R^0 distributions shown in Fig. 2(b) are scaled to the expected rate [7,8] for R^0's with a lifetime equal to the lifetime of the K_L. Since the shape due to R^0 decay is significantly different from those due to kaon decay, we searched for the R^0 by examining the difference between the $M_{\pi^+\pi^-}$ shape and the shape expected from kaon decays. The data show no deviation in the $M_{\pi^+\pi^-}$ shape that could indicate a contribution from an R^0 decay. Limits on R^0 were obtained using the maximum likelihood fit explained above. There are 10 events with $M_{\pi^+\pi^-} \geq 0.6$ GeV$/c^2$ that are not simulated by K_L decays. These events, which are consistent with residual gas interactions in the vacuum, are treated as signal in the fit.

Various $R^0, \tilde{\gamma}$ combinations, with $1.3 \leq r \leq 2.2$, were used in the fit. All fits yielded R^0 components consistent with zero. An upper limit for a given R^0 was determined by evaluating the maximum-likelihood curve at the 90% confidence level (C.L.) interval, which limited the R^0 decays to less than a few tens to hundreds range. The detector acceptance and the R^0 flux at production were then determined as a function of the R^0 lifetime. The normalization was performed using 2.1×10^6 $K_L \to \pi^+\pi^-$ events observed, from which we determined that 37.7×10^{10} K^0 exited the absorbers [4]. Figure 3 shows the 90% C.L. upper limit on the ratio R^0/K^0, as well as the expectation for the R^0/K^0 ratio for $r = 1.4$.

Figure 4 shows the variation of the 90% C.L. upper limit on the R^0/K^0 flux ratio with the R^0 lifetime for two sample $R^0, \tilde{\gamma}$ combinations. Particles with lifetimes much shorter than the K_L decay too close to the target to be visible in the detector, while those with much longer lifetimes exit the detector without decaying. We use the R^0/K^0 flux expectation to exclude a range of lifetimes for a given $R^0, \tilde{\gamma}$ combination. Figure 5 shows R^0 lifetimes excluded at 90% C.L. for a given mass, assuming a 100% branching fraction for the $R^0 \to \pi^+\pi^-\tilde{\gamma}$ decay. Contours are shown for $r = 1.3$, 1.4, 1.55, and 1.73.

In this analysis, we are able to exclude R^0's with masses well below the lower limits of previous searches ($\sim$2.2 GeV$/c^2$). The lower limit of the exclusion contour (at 1.3 GeV$/c^2$ for $r = 1.3$) is due to the kinematic limit of $M_{R^0} - M_{\tilde{\gamma}} = 2M_\pi$. We note that in the theoretically interesting regions of M_{R^0} and r, our exclusion covers lifetimes as low as 3×10^{-10} sec, and as high as 10^{-3} sec, effectively spanning the theoretically interesting range of lifetimes.

If the mass difference $M_{R^0} - M_{\tilde{\gamma}}$ is less than $2M_\pi$ then the R^0 can decay only via $R^0 \to \pi^0\tilde{\gamma}$. We searched for the decay $R^0 \to \pi^0\tilde{\gamma}$, $\pi^0 \to \gamma\gamma$ in data taken during a special run whose primary purpose was to search for the decay $K_L \to \pi^0\nu\overline{\nu}$ [9]. Since the signatures for the K_L and R^0 decays, two photons with missing transverse momentum (P_T), are similar, these data are sensitive to $R^0 \to \pi^0\tilde{\gamma}$ decays.

Only one narrow beam of neutral kaons was used in this run, with the transverse beam size of 4 cm $\times$ 4 cm at the calorimeter. The trigger was designed to select events with two energy clusters in the calorimeter, together with four cluster events ($K_L \to \pi^0\pi^0$) for normalization. The longitudinal distance of the decay vertex from the target (Z) and the transverse momentum of the two photons were determined by constraining the invariant mass of the two photons to that of π^0. The average P_T resolution was $\sim$8 MeV$/c$. The selection criteria used in this data sample are similar to the one used in the $\pi^0\nu\overline{\nu}$ analysis [9], with the exception of the P_T cut at 260 MeV$/c$. Photon veto detectors and drift chambers were used to suppress backgrounds from other kaon decays and hadronic interactions in the detector. The events were required to have the decay vertex in vacuum, with the vertex Z position in the range $125 \leq Z \leq 157$ m.

We examined the shape of the P_T distribution to isolate R^0 candidates. The P_T distribution of the final data sample is shown in Fig. 6, along with the background expected from $K_L \to \gamma\gamma$ and $\Lambda \to n\pi^0$ decays. The peak near $P_T = 0$ is from the decay $K_L \to \gamma\gamma$, and the remaining events below $P_T = 160$ MeV$/c$ are from Λ decays. The signal search region is at $P_T > 160$ MeV$/c$. This value for the P_T cut is the same as the lower P_T cut used in the $K_L \to \pi^0\nu\overline{\nu}$ analysis. It was chosen to minimize background from hyperon and K_L decays by

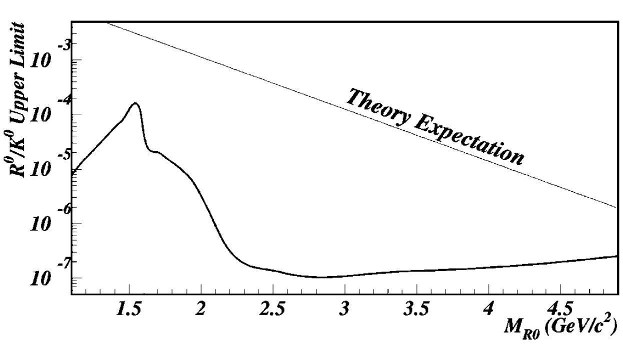

FIG. 3. The 90% C.L. upper limit on the R^0/K^0 ratio, and the expectation, for $r = 1.4$, $\tau(R^0) = 5 \times 10^{-8}$ sec .

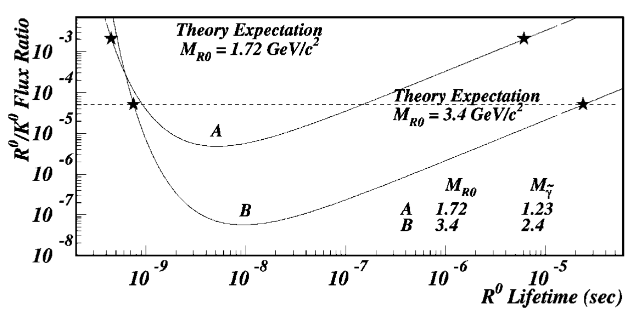

FIG. 4. Upper limits with 90% C.L. on the R^0/K^0 flux ratio as a function of R^0 lifetime, for two M_{R^0}, $M_{\tilde{\gamma}}$ combinations, with masses listed in GeV$/c^2$. The dotted lines show the expectation for the flux ratio, and the stars mark the corresponding lifetime limits.

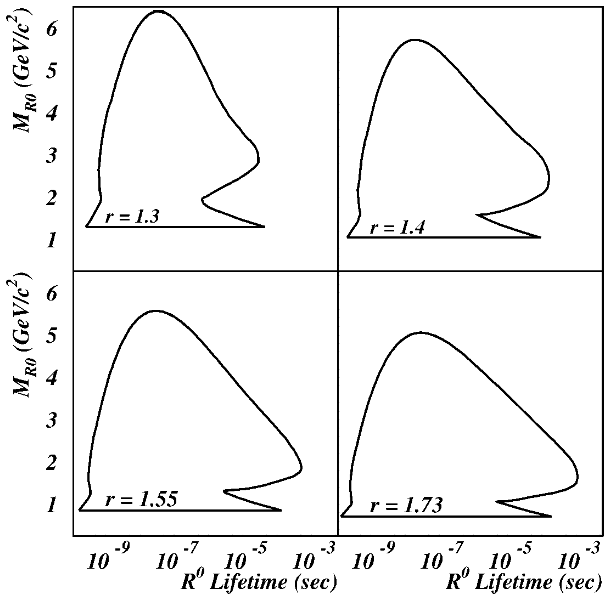

FIG. 5. R^0 mass-lifetime regions excluded at 90% C.L., for the decay $R^0 \rightarrow \pi^+\pi^-\tilde{\gamma}$, for values of $r = 1.3$, 1.4, 1.55, and 1.73. The lower edges are due to the kinematic limit of $M_{R^0} - M_{\tilde{\gamma}} = 2M_\pi$.

examining the relevant background Monte Carlo distributions, before the data were examined. Clearly, we are sensitive to R^0 masses for which the $\pi^+\pi^-$ decay cannot proceed.

The backgrounds due to neutron interactions with material such as the vacuum window or drift chambers were not simulated. At $P_T \geq 130$ MeV/c, these interactions dominate the data as backgrounds due to hyperons and K_L decays diminish. These interactions can produce two photons in the calorimeter, for instance, from an η or from different pions in a multi-π^0 event. For such events, the vertex position may be misreconstructed within the fiducial region of the analysis due to the assumption that the two detected photons originated from the decay of a single π^0.

We have determined the neutron rejection efficiency of the detector using a sample of neutrons from $\Lambda \rightarrow n\pi^0$ decays in a manner similar to the one described in [9]. The number of events with high P_T seen in the data is consistent with that expected from interactions due to neutron rejection inefficiency. After all cuts, two events remain in the signal region with $P_T > 160$ MeV/c. We expect the number of events from hadronic interactions to be 4.7 ± 1. Treating these two events as signal, the corresponding 90% C.L. upper limit on the number of observed R^0 signal events is 5.32.

The K_L flux in this data sample was measured from 3466 observed $K_L \rightarrow \pi^0\pi^0$ decays. The pQCD prediction for the R^0/K_L flux ratio was used as before to obtain upper and lower lifetime limits at the 90% C.L., assuming the R^0 decays 100% of the time to $\pi^0\tilde{\gamma}$. Figure 7 shows the exclusion contours for $r = 1.3$, and $r = 1.4$ using the π^0 analysis, and the $\pi^+\pi^-$ analysis. Note that using the π^0 analysis, we extend the range of excluded M_{R^0} down to 0.8 GeV/c^2, for lifetimes between 2.5×10^{-10} and 5.6×10^{-6} sec.

The analyses presented in this paper exclude most R^0 masses, over six decades in a lifetime. A significant portion of the region allowed by the cosmological constraint $r \leq 1.4$ and $M_{R^0} \leq 2.2$ GeV/c^2 which was not addressed by previous searches is now excluded. We thus definitively rule out the long-standing light gluino models advocated by Farrar, Raby, and others [1,2]. Our null results eliminate most SUSY models in which gauginos remain massless at tree level. More generally, our understanding of the $M_{\pi^+\pi^-}$ shape will constrain future models that predict long-lived particles with a $\pi^+\pi^-$ component in their decays.

We thank Glennys Farrar for suggesting this search and for discussions concerning this work and, along

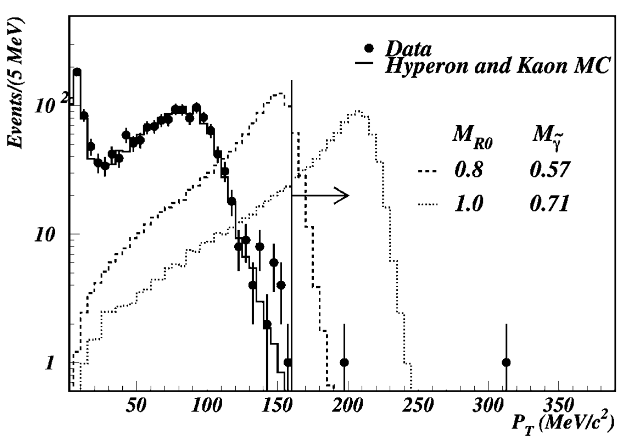

FIG. 6. The P_T distribution for $\gamma\gamma$ events from the narrow-beam run (dots). The background from K_L and hyperon decays is shown by the solid line. The arrow indicates the R^0 signal region. The MC simulations for $M_{R^0} = 0.8, 1.0$ GeV/c^2 (dashed, dotted lines) are also shown, both for $r = 1.4$.

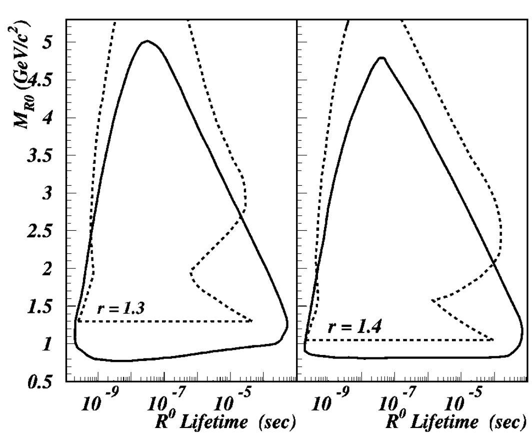

FIG. 7. R^0 mass-lifetime regions excluded using pQCD for $r = 1.3$ and 1.4. The exclusion from the π^0 analysis (solid lines) and $\pi^+\pi^-$ (dashed lines) analysis is shown.

with Rocky Kolb, for pointing out the cosmological significance of this search. We gratefully acknowledge the support and effort of the Fermilab staff and the technical staffs of the participating institutions for their vital contributions. This work was supported in part by the U.S. DOE, The National Science Foundation, and The Ministry of Education and Science of Japan. In addition, A. R. B., E. B., and S. V. S. acknowledge support from the NYI program of the NSF; A. R. B. and E. B. from the Alfred P. Sloan Foundation; E. B. from the OJI program of the DOE; and K. H., T. N., and M. S. from the Japan Society for the Promotion of Science.

*To whom correspondence should be addressed. Electronic address: lath@physics.rutgers.edu

†On leave from C.P.P. Marseille/C.N.R.S., France.

[1] R. N. Mohapatra and S. Nandi, Phys. Rev. Lett. **79**, 181 (1997); Z. Chacko *et al.*, Phys. Rev. D **56**, 5466 (1997); S. Raby, Phys. Rev. D **56**, 2852 (1997).

[2] G. R. Farrar, Phys. Rev. Lett. **76**, 4111 (1996); Phys. Rev. D **51**, 3904 (1995).

[3] D. J. H. Chung, G. R. Farrar, and E. W. Kolb, Phys. Rev. D **56**, 6096 (1997); G. R. Farrar and E. W. Kolb, Phys. Rev. D **53**, 2990 (1996).

[4] J. Adams *et al.*, Phys. Rev. Lett. **79**, 4083 (1997).

[5] G. R. Farrar, Nucl. Phys. (Proc. Suppl.) **62**, 485 (1998) (available as e-print hep-ph/9710277).

[6] V. Fanti *et al.*, Phys. Lett. B **446**, 117 (1999).

[7] S. Dawson, E. Eichten, and C. Quigg, Phys. Rev. D **31**, 1581 (1985).

[8] C. Quigg (private communication).

[9] J. Adams *et al.*, Phys. Lett. B **447**, 240 (1999).